Macromolecular Research, Vol. 16, No. 8, pp 686-694 (2008)

# X-Ray Scattering Studies on Molecular Structures of Star and Dendritic Polymers

**Sangwoo Jin, Kyeong Sik Jin, Jinhwan Yoon, Kyuyoung Heo, Jehan Kim, Kwang-Woo Kim, and Moonhor Ree***

*Department of Chemistry, National Research Lab for Polymer Synthesis & Physics, Pohang Accelerator Laboratory, Center for Integrated Molecular Systems, Polymer Research Institute, and BK school of Molecular Science, Pohang University of Science and Technology, Pohang 790-784, Korea*

**Tomoya Higashihara, Takumi Watanabe, and Akira Hirao***

*Polymeric and Organic Materials Department, Graduate School of Science and Engineering, Tokyo Institute of Technology, H-127, 2-12-1, Ohokayama, Meguro-ku, Tokyo 152-8552, Japan*

*Received March 23, 2008; Revised May 3, 2008; Accepted May 6, 2008*

**Abstract:** We studied the molecular shapes and structural characteristics of a 33-armed, star polystyrene (PS-33A) and two 3rd-generation, dendrimer-like, star-branched poly(methyl methacrylate)s with different architectures (PMMA-G3a and PMMA-3Gb) and 32 end-branches under good solvent and theta ($\Theta$) solvent conditions by using synchrotron small angle X-ray scattering (SAXS). The SAXS analyses were used to determine the structural details of the star PS and dendrimer-like, star-branched PMMA polymers. PS-33A had a fuzzy-spherical shape, whereas PMMA-G3a and PMMA-G3b had fuzzy-ellipsoidal shapes of similar size, despite their different chemical architectures. The star PS polymer's arms were more extended than those of linear polystyrene. Furthermore, the branches of the dendrimer-like, star-branched polymers were more extended than those of the star PS polymer, despite having almost the same number of branches as PS-33A. The differences between the internal chain structures of these materials was attributed to their different chemical architectures.

*Keywords*: 33-armed star polystyrene, 3rd-generation dendrimer-like star-branched poly(methyl methacrylate)s, small angle X-ray scattering, molecular shape, internal chain structure, good solvent condition, theta solvent condition.

## Introduction

Branched polymers, including brush, star and dendritic polymers have many branches that give them high connectivity and functionality, and thus they are of significant interest to academia and industry.[1-11] In particular, star polymers and dendrimer-like star-branched polymers belong to the class of well-defined hyperbranched macromolecules. Much research effort has been expended over the last three decades in the synthesis of star and dendritic polymers and the characterization of their structures and properties. As a result, various star and dendritic polymers have been described with reports of their structures and properties.[12,13] However, these studies were limited to star and dendritic polymers with relatively low numbers of arms and branches until the early 1990s, because of difficulties in their synthesis.[12,13] Moreover, their structural analyses have been limited to determinations of their molecular sizes.

*Corresponding Authors. E-mails: ree@postech.edu or ahirao@polymer.titech.ac.jp

Dendrimer-like star-branched polymers, which consist of an integrated system of star and dendritic polymers, have recently been introduced.[14] These polymers can have various architectures and functionalities even though they are in the same generation,[15,16] and have thus attracted significant attention as a new class of dendrimers. However, their molecular shapes and structural properties have not yet been studied in detail.

In the present study, we synthesized a 33-armed star polystyrene (PS-33A) and two 3rd-generation dendrimer-like star-branched poly(methyl methacrylate)s with 32 end-branches and different architectures (PMMA-G3a and PMMA-3Gb) (see Figure 1), and characterized them in under good solvent and theta ($\Theta$) solvent conditions by using synchrotron small angle X-ray scattering (SAXS). The measured SAXS profiles were quantitatively analyzed by using various structural model techniques and a structural model free method. The SAXS analyses were used to determine the structural details (size, shape, and internal structure) of the star and dendrimer-like star-branched polymers. In particular, under both good and $\Theta$

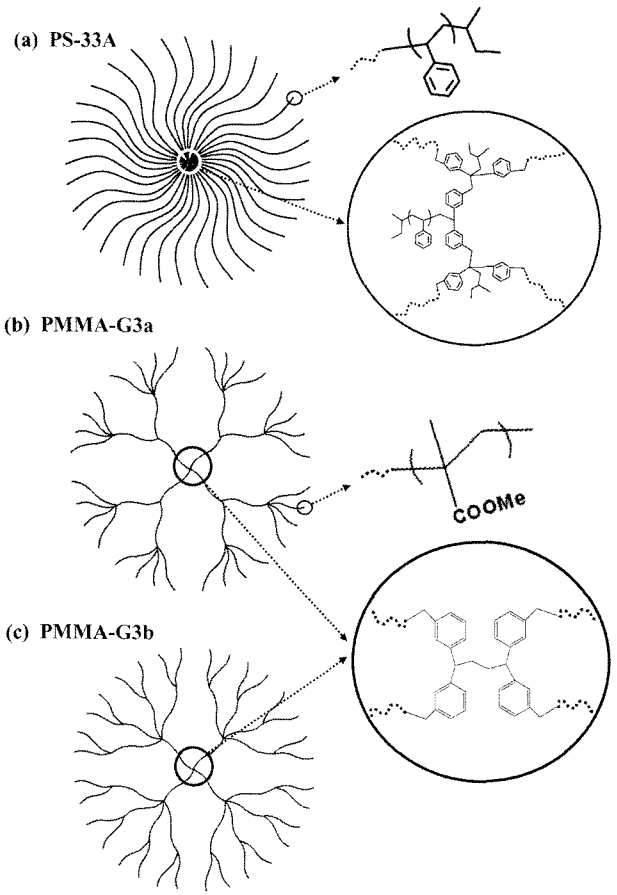


**Figure 1.** Structures of the 33-armed star PS (PS-33A) and the two 3rd-generation dendrimer-like star-branched PMMAs (PMMA-G3a and PMMA-G3b).

solvent conditions, PS-33A was determined to have a fuzzy-spherical shape whereas both PMMA-G3a and PMMA-3Gb were surprisingly found to have a fuzzy-ellipsoidal shape rather than a spherical shape, even though they have almost the same number of branches as PS-33A.

## Experimental

PS-33A was synthesized by coupling reaction of polymer anions consisting of two polymer chains with chain-end-multifunctionalized polystyrenes with benzyl bromide moieties as reported previously in the literature.[17] PMMA-G3a and PMMA-G3a were synthesized by repeating the two reactions involving a linking reaction of pre-made living anionic PMMA with either two or four 3-*tert*-butyldimethylsilyloxymethylphenyl groups with chain-end-functionalized PMMAs.[6,13,15] In addition, a linear PS was purchased from Varian Inc. All other chemicals were supplied from Aldrich Chemical Co. The weight- and number-average molecular weights ($\overline{M}_w$ and $\overline{M}_n$) of all the polymers were measured by using vapor pressure osmometry and static light scattering.[6,13,15,17] The $\overline{M}_w$ and $\overline{M}_n$ results are summarized in Table I. For each polymer sample, 1.0 wt% solutions were prepared in a good and a $\Theta$ solvent conditions: tetrahydrofuran (THF) at 25 °C was chosen as a good solvent condition for all the polymers while cyclohexane at 35 °C was used as a $\Theta$ solvent condition for the linear and star PS polymers and 4-heptanone at 25 °C was chosen as a $\Theta$ solvent condition for the PMMA-G3a and PMMA-G3a polymers.

**Table I. Weight- and Number-Average Molecular Weights of the Linear, Star, and Dendrimer-Like Star-Branched Polymers Investigated in this Study**

| Sample | Type | $\overline{M}_w$ | $\overline{M}_w/\overline{M}_n$ |
|---|---|---|---|
| Linear PS | Linear | 43,900 | 1.01 |
| PS-33A | Star | 186,000 | 1.03 |
| PMMA-G3a | Dendrimer: $(A\text{-}A_2\text{-}A_8)_4$ [a] | 514,000 | 1.02 |
| PMMA-G3b | Dendrimer: $(A\text{-}A_4\text{-}A_8)_4$ | 568,000 | 1.03 |

[a]The symbol 'A' denotes a linear type of polymer chain component in the 3rd-generation dendrimer.

SAXS measurements were carried out at the 4C1 SAXS beamline (BL)[18-23] of the Pohang Accelerator Laboratory at the Pohang University of Science and Technology.[24] At the 4C1 BL, a light source from a bending magnet of the Pohang Light Source storage ring was focused with a toroidal silicon mirror coated with platinum and monochromatized with a $W/B_4C$ double multiplayer monochromator, giving an X-ray beam of wavelength 1.608 Å. The X-ray beam size at the sample stage was 0.6×0.6 mm$^2$. A two-dimensional (2D) charge-coupled detector (CCD) (Mar USA, Inc.) was employed. The sample-to-detector distances of 1.0, 2.0 and 3.0 m were used. The scattering angle was calibrated with linear polyethylene, collagen (chicken tendon), and polystyrene-*b*-polyethylene-*b*-polybutadiene-*b*-polystyrene standards. We used solution sample cells with 10 $\mu$m thick mica windows and an X-ray beam path length of 0.7 mm. Each 2D SAXS pattern was circular averaged from the beam center, then normalized to the transmitted X-ray beam intensity, which was monitored with a scintillation counter placed behind the sample, and corrected for the scattering due to the used solvent.

## Results and Discussion

The scattering intensity $I(q)$ from globular particles in a solvent medium can be expressed in the following:[18,23,25-29]

$$I(q) = kNP(q)S(q) \quad (1)$$

where $k$ is a constant, $N$ is the number of particles, $P(q)$ is the form factor of single particle, and $S(q)$ is the structure factor: here $q$ is the magnitude of scattering vector which is defined by $q = 4\pi \sin\theta/\lambda$ where $2\theta$ is the scattering angle.

The term $P(q)$ provides information on the particle shape and size while the term $S(q)$ provides the inter-particle distances in the solution. In general, for dilute solutions the term $S(q)$ can be approximated to unity over the entire $q$ range, and indeed the term $P(q)$ can be directly obtained from the scattering intensity $I(q)$, providing the particle shape and size. Taking these facts into account, the scattering profiles were obtained in dilute conditions for each case, and analyzed quantitatively to determine the exact molecular shapes and polymeric segmental behaviors of the polymers.

**Linear PS.** The scattering profiles measured for the linear PS in both the solvent conditions are presented in Figure 2. For the linear PS in a given solution condition, the average radius of gyration ($\overline{R_g}$) is determined from the scattering intensity profile in the low $q$ region satisfying a condition $q\overline{R_g} < 1.0$ by using the Guinier analysis:[18,23,25,28,29]

$$\ln I(q) = \ln I_o(q) - \overline{R_g}^2 q^2/3 \quad (2)$$

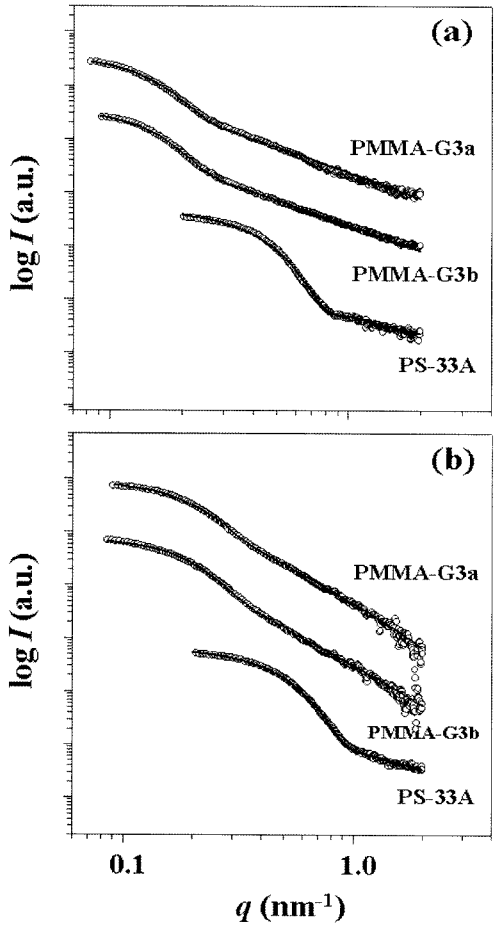


**Figure 2.** X-ray scattering profiles of the star PS and the 3rd-generation dendrimer-like star-branched PMMAs obtained under (a) good and (b) $\Theta$ solvent conditions. The symbols are the measured data, and the solid lines were obtained by fitting the data with a fuzzy-sphere for the star PS and a fuzzy-ellipsoid for the dendrimer-like star-branched PMMAs.

where $I(q)$ and $I_o(q)$ are the scattering intensity and the incident beam intensity respectively.

The Guinier analysis found that the linear PS reveals $\overline{R_g}$ = 59 Å in the good solvent condition and $\overline{R_g}$ =50 Å in the $\Theta$ solvent condition (Table II) as commonly observed for flexible linear polymers. Furthermore, the scattering profile measured in the good solvent condition follows a $q^{-5/3}$ power law in the intermediate $q$ region as well as in the high $q$ region. On the other hand, the scattering profile measured in the $\Theta$ solvent condition follows a $q^{-2}$ power law in the intermediate and in the high $q$ region. Collectively these scattering characteristics indicate that the linear PS has a Gaussian spherical shape. Furthermore, the scattering characteristics indicate that the linear PS in the good solvent condition is a worm-like polymer chain undergoing a self-avoiding random walk while that in the $\Theta$ solvent is a Gaussian polymer chain revealing an excluded volume effect.[29] These results are in good agreement with those previously reported in the literature.[29]

**Star PS.** The scattering profiles of PS-33A obtained for both solvent conditions are displayed in Figure 2. We found with a Guinier analysis of the scattering profiles that the star PS polymer exhibits $\overline{R_g}$=45.0 Å under good solvent conditions and $\overline{R_g}$=39.6 Å under $\Theta$ solvent conditions (Table II). Thus this star polymer expands in the good solvent but contracts in the $\Theta$ solvent, as observed for flexible, linear PS. As shown in Figure 2, these scattering profiles are quite different from those of linear PS. In the intermediate $q$ region, the scattering profiles decay more rapidly than those of linear PS. In the intermediate $q$ region, the scattering profiles for PS-33A in both solvents contain a decay that nearly follows a $q^{-4}$ power law, rather than the $q^{-5/3}$ and $q^{-2}$ power laws observed for linear PS under good and $\Theta$ solvent conditions. However, in the high $q$ region, the scattering profile measured under the good solvent conditions follows a $q^{-5/3}$ power law, whereas that for the $\Theta$ solvent conditions obeys a $q^{-2}$ power law, as observed for linear PS. These results indicate that the molecular shape of PS-33A is close to spherical, quite different from that of linear PS, which exhibits a Gaussian spherical shape. However, the star PS polymer still exhibits the same segmental characteristics as observed for flexible, linear PS. Moreover, the star PS polymer does not have as sharp an interface with the solvent as observed for hard sphere particles. Thus the PS-33A polymer has a spherical shape with "fuzziness".

Cyclohexane at 35 °C was used in our study as the $\Theta$ solvent conditions; note however that these are the $\Theta$ solvent conditions for linear PS rather than the star PS polymer. In general, the $\Theta$ temperature of dendritic polymers can be lower or higher than that of the corresponding linear polymer, depending on the number and length of the branches.[30] Thus the chosen $\Theta$ solvent conditions might be somewhat different from those of the PS-33A polymer. Nevertheless the $\Theta$ solvent conditions chosen in this study

**Table II. Structural Parameters Obtained from the Analyses of the X-ray Scattering Data by Using Fuzzy-Sphere and Ellipsoid Models**

| Sample | Good Solvent Condition ($\Theta$ Solvent Condition) | | | | | | | | | |
|---|---|---|---|---|---|---|---|---|---|---|
| | | Fuzzy-Sphere | | | | Fuzzy-Ellipsoid | | | | |
| | $\overline{R_g}$ [a] (Å) | $R_{g,sc}$ [b] (Å) | $2\sigma_{f,s}$ [c] (Å) | $\frac{\sigma_{f,s}}{R_{g,sc}}$ [d] | $\bar{\xi}$ [e] (Å) | $R_{g,ec}$ [f] (Å) | $2\sigma_{f,e}$ [g] (Å) | $\frac{\sigma_{f,e}}{R_{g,ec}}$ [h] | $\varepsilon$ [i] | $\bar{\xi}$ (Å) |
| Linear PS | 59.0 (50.0) | | | | | | | | | |
| PS-33A | 45.0 (39.6) | 34.9 (30.7) | 21.6 (18.4) | 0.31 (0.30) | 23 (21) | | | | | |
| PMMA-G3a | 127.6 (90.4) | | | | | 118.4 (85.7) | 73.4 (51.4) | 0.31 (0.30) | 0.54 (0.49) | 71 (56) |
| PMMA-G3b | 124.7 (94.6) | | | | | 117.9 (89.1) | 70.4 (53.5) | 0.30 (0.30) | 0.55 (0.49) | 71 (57) |

[a]Average radius of gyration obtained from the Guinier fits. [b]Radius of gyration of the spherical core obtained from the analysis of the measured scattering data with a fuzzy-sphere model. [c]Thickness of the soft shell part obtained from the analysis of the measured scattering data with a fuzzy-sphere model. [d]Fuzziness, which is the ratio of the half thickness $\sigma_{f,s}$ of soft shell region and the radius of gyration $R_{g,sc}$ of the sphere core. [e] $\bar{\xi}$ is the average correlation length of density fluctuation. [f]Radius of gyration of the ellipsoidal core obtained from the analysis of the measured scattering data with a fuzzy-ellipsoid model. [g]Thickness of the soft shell part obtained from the analysis of the measured scattering data with a fuzzy-ellipsoid model. [h]Fuzziness, which is the ratio of the half thickness $\sigma_{f,e}$ of soft shell region and the radius of gyration $R_{g,ec}$ of the ellipsoid core. [i]Aspect ratio, which is the ratio of the long axis and the short axis in the fuzzy-ellipsoidal dendrimer.

are likely to approximate the $\Theta$ solvent conditions of PS-33A.

The scattering profiles were further analyzed by using indirect Fourier transform (IFT) method because this technique has some great advantages as follows. The IFT method does not need any scattering model for analyzing the scattering data and is further able to minimize the effects of missing data. Thus, this technique accurately provides both the pair distance distribution function $p(r)$ and the radial electron density distribution function $\rho(r)$ where $r$ is the distance between the paired scattering elements in the polymer molecule.[23,28,31] The molecular shape in each solvent condition can be obtainable from the pair correlation function $p(r)$ related to the radial electron density distribution function $\rho(r)$:

$$p(r) = r^2 \int_{-\infty}^{\infty} \rho(r)\rho(x-r)dx \quad (3)$$

As can be seen in Figure 3, in both the solvent conditions the $p(r)$ functions show a symmetrical shape and their maximum approaches to $r/\overline{R_g} \approx 1.36$. In general, a homogeneous sphere reveals a $P(r)$ in a symmetrical shape and its $p(r)$ shows a maximum value at $r/R_g \approx 1.36$.[32] Taking this fact into account, the IFT analysis results confirm that the PS-33A reveals a spherical molecular shape in the solvent condition as well as in the $\Theta$ solvent condition.

In general, the scattering form factor of a polymer chain in the intermediate $q$ region is dominated by its molecular shape, while its scattering form factor in the high $q$ region is dominated by density fluctuations on length scales smaller than its dimension (namely, its internal chain structure). Taking this fact into account, the scattering profile in the high $q$ region of PS-33A is attributed to its internal chain structures. The internal chain structures can be described as a specific chain consisting of "blobs":[33] the blob is a spherical volume with a radius $\xi$ where $\xi$ is the correlation length

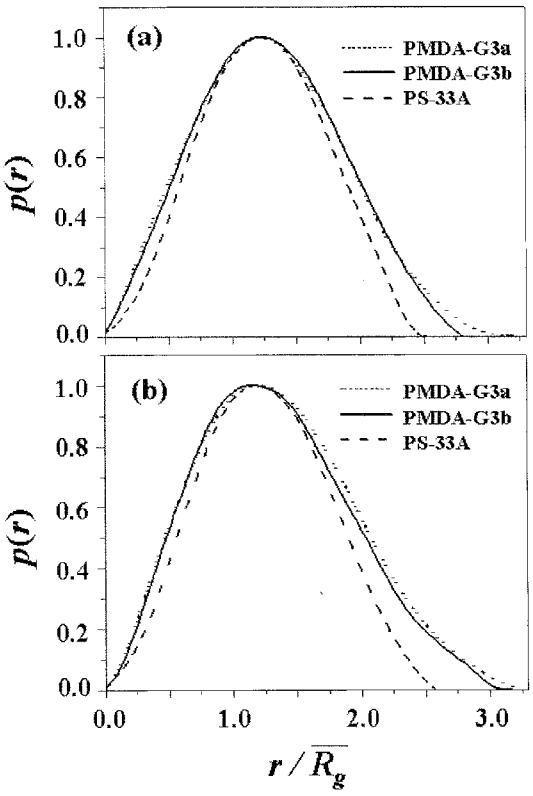


**Figure 3.** Pair distance distribution functions $p(r)$ of star PS and the 3rd-generation dendrimer-like star-branched PMMAs under (a) good and (b) $\Theta$ solvent conditions determined from the analysis of the measured X-ray scattering data using the IFT method. The x-axis is normalized to the $3\overline{R_g}$ value determined from the Guinier analysis of the measured scattering data.

of density fluctuation. Therefore, the scattering form factor $P(q)$ of PS-33A can be described by a functional description of the form factor that is just the sum of two terms in the

following equation:[32]

$$P(q) = P_{shape}(q) + 4\pi\alpha\int_0^{\bar{\xi}} r^2\gamma(r)\frac{\sin(qr)}{qr}dr \quad (4)$$

where the first term $P_{shape}(q)$ is the form factor from the overall shape of PS-33A and the second term [i.e., $P_{blob}(q)$] is the Fourier transform of the correlation function $\gamma(r)$ of density fluctuations on length scales ($r$) smaller than the blob' radius, $\alpha$ is the amplitude of the blob scattering contribution, and $\bar{\xi}$ is the average correlation length. $\gamma(r)$ is equal to zero for $r > \bar{\xi}$, but not equal to zero for $r \le \bar{\xi}$. For $r \le \bar{\xi}$, $\gamma(r)$ can be expressed by

$$\gamma(r) \propto r^{\mu-2} \quad (5a)$$

$$\mu = \nu^{-1} - 1 \quad (5b)$$

where $\nu$ is the Flory-Huggins parameter, which equals 3/5 for the good solvent condition, 1/2 for the $\Theta$ solvent condition, and 2/3 in the case that the molecules are stretched.[33]

In eq. (4), a sphere with a fuzziness (i.e., fuzzy-sphere) is applied for the form factor $P_{shape}(q)$ of PS-33A; here, the fuzzy-sphere is consisted of two different parts, namely spherical core and soft shell region. For the fuzzy-sphere, $P_{shape}(q)$ can be replaced by the following equation:[32]

$$P_f^{sph}(q, R_f, \sigma_{f,s}) = A_f^{sph}(q, R_f, \sigma_{f,s})^2 \quad (6a)$$

where

$$A_f^{sph}(q, R_f, \sigma_{f,s}) = A_{sphere}(q, R_f)\exp\left(-\frac{q^2\sigma_{f,s}^2}{4}\right) \quad (6b)$$

Here, $R_f$ is the radius of spherical core, which is relative with the radius of gyration of the spherical core by $R_{g,sc} = \sqrt{3/5}R_f$, $2\sigma_{f,s}$ is a measure of the width of the soft shell region (i.e., soft shell thickness), and $A_{sphere}$ is the scattering amplitude of the hard sphere with the same mass and core density. Further, the fuzziness of the sphere is defined by the ratio of $\sigma_{f,ss}$ and $R_{g,sc}$. The scattering amplitude of the hard sphere can be described by the following equation:[29]

$$A_{sphere}(q, R_f) = \frac{3}{(qR_f)^3}[\sin(qR_f) - qr\cos(qR_f)] \quad (7)$$

Using the above fuzzy-sphere model, we attempted to analyze the measured scattering profiles. The analysis was also attempted with various other structural models. As shown in Figure 2, the scattering data measured under both solvent conditions are satisfactorily fitted with the fuzzy-sphere model. The structural parameters determined from this analysis are summarized in Table II. The analysis results confirm that PS-33A has a fuzzy-spherical shape that consists of a spherical core and a shell under both good and $\Theta$ solvent conditions. As listed in Table II, the fuzzy-spherical PS-33A was determined under good solvent conditions to have a core radius $R_{g,sc}$ of 34.9 Å and a shell thickness $2\sigma_{f,s}$ of 21.6 Å. The fuzzy-sphere polymer is estimated from these values to have a radius of gyration of 56.5 Å. This radius of gyration value is larger than that obtained from the Guinier analysis of the scattering profile. The radius of gyration obtained with the Guinier analysis is almost equal to the sum of the $R_{g,sc}$ and $\sigma_{f,s}$ values; this result suggests that only half of the fuzzy portion (i.e., the soft shell region) of the PS-33A polymer, which has an electron density greater than the other region, is taken into account by the Guinier analysis of the scattering data. Similar results and trends were observed for the star PS polymer under $\Theta$ solvent conditions (Table II). However, all the structural parameters for the $\Theta$ solvent conditions are slightly smaller than those obtained for the good solvent conditions.

We now discuss the internal structure characteristics of the star PS polymer. The average correlation length $\bar{\xi}$, which is the average radius of the blobs in the PS-33A polymer (i.e., a measure of the internal structure characteristics of PS-33A), was found to be 23 Å for the good solvent conditions and 21 Å for the $\Theta$ solvent conditions (Table II). These $\bar{\xi}$ values are approximately four times larger than those (which correspond to 3 to 4 statistical segments) measured for linear PS polymers under good and $\Theta$ solvent conditions.[34]

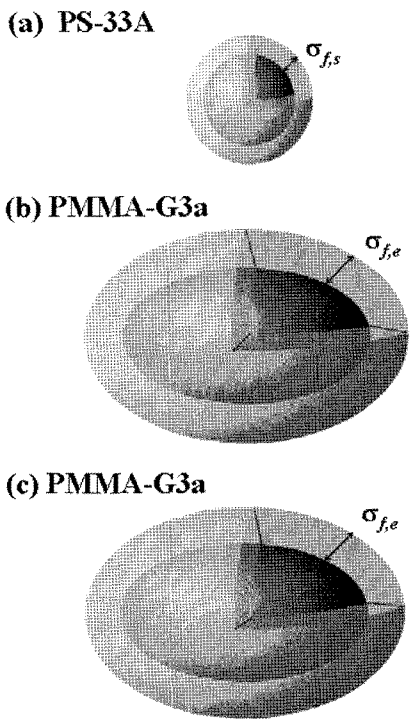


**Figure 4.** Three-dimensional molecular shapes of the star PS and the dendrimer-like star-branched PMMAs under good solvent conditions; the structural parameters were determined from the analysis of the X-ray scattering data: (a) PS-33A; (b) PMMA-G3a; (c) PMMA-G3b. Here, $\sigma_{f,s}$ is the half thickness of the soft shell region in the fuzzy-sphere while $\sigma_{f,e}$ is the half thickness of the soft shell region in the fuzzy-ellipsoid.

These results indicate that under good and $\Theta$ solvent conditions the individual polymer chains of the PS-33A polymer are in a more extended form than is the case for the linear PS chain. The extended chain characteristics of the star polymer might be due to the crowding of the molecular volume with 33 polymer chains.

The three-dimensional (3D) molecular shape of PS-33A under good solvent conditions was determined from the analysis results and is shown in Figure 4. For the $\Theta$ solvent conditions, the molecular shape is similar to that for the good solvent conditions although the molecular size is smaller.

**Dendrimer-Like Star-Branched PMMAs.** The scattering profiles of PMMA-G3a and PMMA-G3b, which were measured under good solvent and $\Theta$ solvent conditions, are shown in Figure 2. As can be seen in the figure, the scattering of PMMA-G3a is very similar to that of PMMA-G3b, suggesting that they have similar molecular shapes and sizes even though their branch architectures and molecular weights are different. Moreover, the scattering profiles contain smoother decays and shifts to low $q$ region than found for the star PS (i.e., PS-33A) (Figure 2). These results show that for given solvent conditions (i.e., good or $\Theta$ solvent conditions) PMMA-G3a and PMMA-G3b have larger molecular sizes than PS-33A, but that their molecular shapes are somewhat different from the spherical form of PS-33A. In the high $q$ region, the scattering profiles for the good solvent conditions follow a $q^{-5/3}$ power law, whereas those obtained under the $\Theta$ solvent conditions obey a $q^{-2}$ power law. These results show that both PMMA-G3a and PMMA-G3b have a molecular shape somewhat deviated from a spherical form, but still exhibit segmental characteristics similar to those observed for flexible, linear polymers. Further, they exhibit no sharp interface with the solvent molecules, as is observed for the flexible, linear PS and the star PS. Thus both the PMMA-G3a and PMMA-G3b polymers have a fuzzy molecular shape. The molecular sizes were determined from the scattering profiles with Guinier analysis. The molecular sizes of the PMMA-G3a and PMMA-G3b polymers are larger under good solvent conditions than under $\Theta$ solvent conditions, as observed for flexible, linear PS, and the star PS. These results are summarized in Table II.

4-Heptanone at 25 °C was used in our study as the $\Theta$ solvent conditions; note however that these are the $\Theta$ solvent conditions for flexible, linear PMMA rather than for dendrimer-like branched PMMA polymers.[30] Nevertheless the $\Theta$ solvent conditions chosen in this study probably approximate the $\Theta$ solvent conditions of PMMA-G3a and PMMA-G3b.

To obtain more information about the molecular shapes of these polymers, the scattering profiles were further analyzed with the IFT method. The obtained $p(r)$ profiles are presented in Figure 3. The $p(r)$ profiles of PMMA-G3a under good and $\Theta$ solvent conditions are similar to those of PMMA-G3b, again confirming that the dendrimer-like PMMA polymers have similar molecular shapes. For both solvent conditions, the $p(r)$ functions have a slightly asymmetrical shape and their maxima appear at $r/\overline{R_g}$ values that are slightly deviated from the value for a sphere of $r/R_g = 1.36$.[32] These IFT analyses confirm that the PMMA-G3a and PMMA-G3b polymers have molecular shapes that are slightly deviated from a spherical form.

Taking these results into account, we attempted to further analyze the measured scattering profiles by using a fuzzy-ellipsoidal model. For a fuzzy-ellipsoid consisting of a core and a soft shell, $P_{shape}(q)$ in eq. (4) can be expressed by an ellipsoidal form factor. The form factor of a rotational ellipsoidal core with the main axes $R_m$ (i.e., a long axis) and $\varepsilon R_m$ (i.e., a short axis; $\varepsilon$ is the aspect ratio) can be expressed by[35]

$$P_{core}^{ell}(q, \varepsilon, R_m) = \int_0^{\pi/2} P_{sphere}(q, r)\sin\alpha d\alpha \tag{8a}$$

where

$$r = R_m\sqrt{\sin^2\alpha + \varepsilon^2\cos^2\alpha} \tag{8b}$$

In eq. (8a), the $P_{shape}(q, r)$ can be expressed by

$$P_f^{ell}(q, \varepsilon, R_m, \sigma_{f,e}) = A_f^{ell}(q, \varepsilon, R_m, \sigma_{f,e})^2 \tag{9a}$$

where

$$A_f^{ell}(q, \varepsilon, R_m, \sigma_{f,e}) = A_{core}^{ell}(q, \varepsilon, R_m)\exp\left(-\frac{q^2\sigma_{f,e}^2}{4}\right) \tag{9b}$$

Here $A_{core}^{ell}$ is the scattering amplitude of the ellipsoidal core: $A_{core}^{ell}(q, \varepsilon, R_m)^2 = P_{core}^{ell}(q, \varepsilon, R_m)$. The radius of gyration of the rotational ellipsoidal core ($R_{g,ec}$) is defined by $R_{g,ec} = R_m\sqrt{(2+\varepsilon^2)/5}$.

Using the above fuzzy-ellipsoid model, we attempted to analyze the measured scattering profiles. The analysis was also attempted with various other structural models. As shown in Figure 2, the scattering data measured under both solvent conditions were found to be satisfactorily fitted with a fuzzy-ellipsoid model. The structural parameters we obtained are summarized in Table II. The analysis results confirm that under good and $\Theta$ solvent conditions both PMMA-G3a and PMMA-G3b have a fuzzy-ellipsoidal shape that consists of an ellipsoidal core and a soft shell. As listed in Table II, the fuzzy-ellipsoid structure of PMMA-G3a has an aspect ratio $\varepsilon$ of 0.54 under good solvent conditions, indicating that the molecular shape of PMMA-G3a is far from spherical. The fuzzy-ellipsoid structure was determined under good solvent conditions to have a core radius $R_{g,ec}$ of 118.4 Å and a shell thickness $2\sigma_{f,e}$ of 73.4 Å (Table II). The fuzzy-ellipsoid polymer was estimated from these values to have a radius of gyration of 191.8 Å. This radius of gyration

is larger than that ($\overline{R_g}$=127.6 Å) obtained from the Guinier analysis of the scattering profile. Furthermore, the $\overline{R_g}$ value is smaller than the sum of the $R_{g,ec}$ and $\sigma_{f,e}$ values; this result suggests that only a small portion of the fuzzy region (i.e., the soft shell region) of the PMMA-G3a polymer is taken into account in molecular size determination with the Guinier analysis of the scattering data. Similar results and trends were observed for the dendrimer-like star-branched PMMA polymers under $\Theta$ solvent conditions (Table II). However, all the structural parameters obtained for the $\Theta$ solvent conditions are slightly smaller than those obtained for the good solvent conditions. PMMA-G3b has a molecular shape and structural characteristics that are very similar to those observed for PMMA-G3a, even though their chemical architectures are different. The 3D molecular shapes of the dendrimer-like star branched PMMAs were determined from the analysis results and are shown in Figure 4.

For PMMA-G3a, the average correlation length $\overline{\xi}$ was determined to be 71 Å under good solvent conditions and 56 Å under $\Theta$ solvent conditions (Table II). Similar $\overline{\xi}$ values were obtained for the PMMA-G3b polymer (Table II). These $\overline{\xi}$ values are nine and twelve times larger than those (which correspond to 3 to 4 statistical segments) obtained for linear PMMA polymers under good and $\Theta$ solvent conditions respectively.[36] Furthermore, these $\overline{\xi}$ values are approximately three times larger than those of the star PS polymer. These results indicate that under good and $\Theta$ solvent conditions the individual polymer chains of both the PMMA-G3a and PMMA-G3b polymers are in a more extended form than found for linear PMMA chains or the star PS polymer. The extended chain characteristics of the dendrimer-like star-branched polymers might be due to the crowding of the molecular volume with 32 branches and their branch architecture.

As can be seen in Figure 1 and Table I, PMMA-G3a and PMMA-G3b have different branch architectures as well as slightly different molecular weights. Thus some differences in molecular shape and size are expected. On the other hand, they are expected to have spherical shapes. However, our X-ray scattering study found that they have almost identical molecular shapes and molecular sizes, as discussed above. Moreover, their molecular shapes are surprisingly fuzzy-ellipsoidal rather than spherical. These molecular shapes are quite different from the fuzzy-spherical shape of the star PS polymer. The ellipsoidal molecular shapes might be due to their branch architecture and internal chain structure and some degree of deficiency in the molecular volume filling by the branches. The radii of gyration are two to three times larger than that of the PS-33A polymer. However, their number of branches is only 32, which is almost the same as that of the star PS polymer. Taking these structural parameters into account, we conclude that the molecular volumes of both PMMA-G3a and PMMA-G3b, which only have 32 branches, are not densely filled. In comparison, the star PS polymer has a relatively small radius of gyration and 33 polymer chains and densely fills its molecular volume. Moreover, the PMMA-G3a and PMMA-G3b polymers exhibit highly extended chain characteristics (i.e., relatively rigid chain characteristics), compared to those of the star PS polymer. It is possible that these factors operate cooperatively and result in the ellipsoidal molecular shape of the dendrimer-like star-branched PMMA polymers.

## Conclusions

We prepared PS-33A as a model star polymer with a high chain number and PMMA-G3a and PMMA-G3b as model dendrimer-like star-branched polymers, and quantitatively investigated their molecular structure under good and $\Theta$ solvent conditions by using the SAXS technique with a synchrotron radiation source. The SAXS analyses were used to determine the molecular shape, size, and internal structure of the star PS and dendrimer-like star-branched PMMA polymers. PS-33A was determined to have a fuzzy-spherical shape consisting of core and soft shell regions. The star PS polymer's arms were found to be more extended than linear PS. Both PMMA-G3a and PMMA-G3b were found to have a fuzzy-ellipsoidal shape composed of core and soft shell regions, even though they have different chemical architectures. The branches of the dendrimer-like star-branched polymers are more extended than those of the star PS polymer, even though they have almost the same number of branches. The differences between the internal chain structures of these polymers might be due to their different chemical architectures.

**Acknowledgment.** This study was supported by the Korea Science & Engineering Foundation (Korea-Japan Cooperation Project No. 4000186001), Ministry of Education, Science and Technology (MEST). The work was also supported by the National Research Lab for Polymer Synthesis and Physics and the Center for Integrated Molecular Systems (which were funded by the Korea Science & Engineering Foundation), and by the BK21 Program, MEST. Synchrotron X-ray scattering measurements at Pohang Accelerator Laboratory were supported by MEST and POSCO. The work done at Tokyo Institute of Technology was supported by a grant (B18350060) from a Grant-in-Aid for Scientific Research from the Ministry of Education, Science, Sports, and Culture of Japan and by the Japan-Korea Bilateral Joint Project from Japan Society for the Promotion of Science.

## References

(1) (a) S. I. Kim, M. Ree, T. J. Shin, and J. C. Jung, *J. Polym. Sci. Part A: Polym. Chem.*, **37**, 2909 (1999). (b) S. W. Lee, T. Chang, and M. Ree, *Macromol. Rapid Commun.*, **22**, 941

(2001). (c) B. Chae, S. B. Kim, S. W. Lee, S. I. Kim, W. Choi, B. Lee, M. Ree, K. H. Lee, and J.C. Jung, *Macromolecules*, **35**, 10119 (2002). (d) B. Chae, S.W. Lee, B. Lee, W. Choi, S. B. Kim, Y. M. Jung, J. C. Jung, K. H. Lee, and M. Ree, *J. Phys. Chem. B*, **107**, 11911 (2003). (e) B. Chae, S. W. Lee, Y. M. Jung, M. Ree, and S. B. Kim, *Langmuir*, **19**, 687 (2003). (f) B. Chae, S. W. Lee, B. Lee, W. Choi, S. B. Kim, Y. M. Jung, J. C. Jung, K. H. Lee, and M. Ree, *Langmuir*, **19**, 9459 (2003). (g) B. Chae, S. W. Lee, S. B. Kim, B. Lee, and M. Ree, *Langmuir*, **19**, 6039 (2003). (h) S. W. Lee, S. I. Kim, B. Lee, W. Choi, B. Chae, S. B. Kim, and M. Ree, *Macromolecules*, **36**, 6527 (2003). (i) S. W. Lee, S. I. Kim, B. Lee, H. C. Kim, T. Chang, and M. Ree, *Langmuir*, **19**, 10381 (2003). (j) S. W. Lee, S. J. Lee, S. G. Hahm, T. J. Lee, B. Lee, B. Chae, S. B. Kim, J. C. Jung, W. C. Zin, B. H. Sohn, and M. Ree, *Macromolecules*, **38**, 4331 (2005). (k) S. G. Hahm, T. J. Lee, T. Chang, J. C. Jung, W.-C. Zin, and M. Ree, *Macromolecules*, **39**, 5385 (2006). (l) S. G. Hahm, T. J. Lee, and M. Ree, *Adv. Funct. Mater.*, **17**, 1359 (2007).

(2) H.-C. Kim, J.-S. Kim, S. Baek, and M. Ree, *Macromol. Res.*, **14**, 173 (2006).

(3) (a) J. Yoon, K. S. Jin, H. C. Kim, G. Kim, K. Heo, S. Jin, J. Kim, K.-W. Kim, and M. Ree, *J. Appl. Cryst.*, **40**, 476 (2007). (b) J. Yoon, S. W. Lee, S. Choi, K. Heo, K. S. Jin, S. Jin, G. Kim, J. Kim, K.-W. Kim, H. Kim, and M. Ree, *J. Phys. Chem. B*, **112**, 5338 (2008).

(4) (a) J. F. G. A. Jansen, H. W. I. Peerlings, E. M. M. de Brabander-Van den Berg, and E. W. Meijer, *Angew. Chem. Int. Ed.*, **34**, 1206 (1995). (b) I. Tabakovic, L. L. Miller, R. G. Duan, D. C. Tully, and D. A. Tomalia, *Chem. Mater.*, **9**, 736 (1997). (c) J. L. Hedrick, T. Magbitang, E. F. Cornnor, T. Glauser, W. Volken, and C. L. Hawker, *Chem. Eur. J.*, **8**, 3308 (2002). (d) J. Groll, E. V. Amirgoulova, T. Ameringer, C. D. Heyes, C. Rocker, G. U. Nienhaus, and M. Moller, *J. Am. Chem. Soc.*, **126**, 4234 (2004). (e) S. M. Rele, W. Cui, L. Wang, S. Hou, B. Barr-Zarse, D. Taton, Y. Gnanou, J. D. Esko, and E. L. Chaikof, *J. Am. Chem. Soc.*, **127**, 10132 (2005).

(5) C. Park, M. Rhue, M. Im, and C. Kim, *Macromol. Res.*, **15**, 688 (2007).

(6) A. Hirao, K. Sugiyama, and H. Yokoyama, *Prog. Polym. Sci.*, **32**, 1393 (2007).

(7) Y. C. Shin, K.-Y. Choi, M. Y. Jin, S.-K. Hong, D. Cho, T. Chang, and M. Ree, *Korea Polym. J.*, **9**, 100 (2001).

(8) J.-S. Kim, H.-C. Kim, B. Lee, and M. Ree, *Polymer*, **46**, 7394 (2005).

(9) B. Lee, Y.-H. Park, Y.-T. Hwang, W. Oh, J. Yoon, and M. Ree, *Nat. Mater.*, **4**, 147 (2005).

(10) B. Lee, W. Oh, Y. Hwang, Y.-H. Park, J. Yoon, K. S. Jin, K. Heo, J. Kim, K.-W. Kim, and M. Ree, *Adv. Mater.*, **17**, 696 (2005).

(11) (a) B. Lee, J. Yoon, W. Oh, Y. Hwang, K. Heo, K. S. Jin, J. Kim, K.-W. Kim, and M. Ree, *Macromolecules*, **38**, 3395 (2005). (b) B. Lee, W. Oh, J. Yoon, Y. Hwang, J. Kim, B. G. Landes, J. P. Quintana, and M. Ree, *Macromolecules*, **38**, 8991 (2005). (c) M. Ree, J. Yoon, and K. Heo, *J. Mater. Chem.*, **16**, 685 (2006). (d) Y. Kim, S. Cook, S. M. Tuladhar, S. A. Choulis, J. Nelson, J. R. Durrant, D. D. C. Bradley, M. Giles, I. McCulloch, C.-S. Ha, and M. Ree, *Nat. Mater.*, **5**, 197 (2006). (e) K. Heo, K. S. Jin, J. Yoon, S. Jin, W. Oh, and M. Ree, *J. Phys. Chem. B*, **110**, 15887 (2006). (f) J. Yoon, K. Heo, W. Oh, K. S. Jin, S. Jin, J. Kim, K.-W. Kim, T. Chang, and M. Ree, *Nanotechnology*, **17**, 3490 (2006). (g) K. S. Jin, K. Heo, W. Oh, J. Yoon, B. Lee, Y. Hwang, J.-S. Kim, Y.-H. Park, T. Chang, and M. Ree, *J. Appl. Cryst.*, **40**, s631 (2007). (h) W. Oh, Y. Hwang, T. J. Shin, B. Lee, J.-S. Kim, J. Yoon, S. Brennan, A. Mehta, and M. Ree, *J. Appl. Cryst.*, **40**, s626 (2007). (i) W. Oh, Y. D. Park, Y. Hwang, and M. Ree, *Bull. Korean Chem. Soc.*, **28**, 2481 (2007).

(12) (a) B. J. Bauer and L. J. Fetters, *Rubber Chem. Technol.*, **51**, 406 (1978). (b) J. Roovers, N. Hadjichristidis, and L. J. Fetters, *Macromolecules*, **16**, 214 (1983). (c) J. Roovers, in *Encyclopedia of Polymer Science and Engineering*, 2nd ed., J. I. Kroschwitz, Ed., Wiley-Interscience, New York, 1985, Vol. 2, p. 478. (d) K. Huber, S. Bantle, W. Burchard, and L. J. Fetters, *Macromolecules*, **19**, 1404 (1986). (e) D. Richter, B. Farago, L. J. Fetters, J. S. Huang, and B. Ewen, *Macromolecules*, **23**, 1845 (1990). (f) P. J. Lutz and D. Rein, in *Star and Hyperbranched Polymers*, M. K. Mishra and S. Kobayashi, Eds., Marcel Dekker, New York, 1999, p. 27. (g) N. Hadjichristidis, M. Pitsikalis, S. Pispas, and H. Iatou, *Chem. Rev.*, **101**, 3747 (2001).

(13) A. Hirao, M. Hayashi, S. Loykulnant, K. Sugiyama, S.-W. Ryu, N. Haraguchi, A. Matsuo, and T. Higashihara, *Prog. Polym. Sci.*, **30**, 111 (2005).

(14) S. M. Grayson and M. J. Fréchet, *Chem. Rev.*, **101**, 3619 (2001).

(15) A. Hirao, K. Sugiyama, Y. Tsunoda, A. Matsuo, and T. Watanabe, *J. Polym. Sci. Part A: Polym. Chem.*, **44**, 6659 (2006).

(16) D. Taton, S. Matmour, S. Angot, S. Hou, R. Francis, B. Lepoittevin, D. Moinard, J. Babin, and Y. Gnanou, *Polym. Int.*, **55**, 1138 (2006).

(17) (a) A. Hirao and N. Haraguchi, *Macromolecules*, **35**, 7238 (2002). (b) A. Hirao and Y. Tokuda, *Macromolecules*, **36**, 6081 (2003). (c) A. Hirao, M. Hayashi, S. Loykulnant, K. Sugiyama, S.-W. Ryu, N. Haraguchi, A. Matsuo, and T. Higashihara, *Prog. Polym. Sci.*, **30**, 111 (2005).

(18) J. Bolze, J. Kim, J.-Y. Huang, S. Rah, H. S. Youn, B. Lee, T. J. Shin, and M. Ree, *Macromol. Res.*, **10**, 2 (2002).

(19) (a) M. Ree, S. H. Woo, and T. J. Shin, *Polymer Sci. Technol. (Korea)*, **8**, 57 (1997). (b) M. Ree, S. I. Kim, S. W. Lee, and J. H. Jung, *Polymer Sci. Technol. (Korea)*, **8**, 663 (1997).

(20) M. Ree, T. J. Shin, and S. W. Lee, *Korea Polym. J.*, **9**, 1 (2001).

(21) (a) T. J. Shin, B. Lee, H. S. Youn, K.-B. Lee, and M. Ree, *Langmuir*, **17**, 7842 (2001). (b) B. Lee, T. J. Shin, S. W. Lee, J. W. Lee, and M. Ree, *Macromol. Symp.*, **190**, 173 (2002). (c) B. Lee, T. J. Shin, S. W. Lee, J. Yoon, J. Kim, H. S. Youn, K.-B. Lee, and M. Ree, *Polymer*, **44**, 2509 (2003). (d) B. Lee, T. J. Shin, S. W. Lee, J. Yoon, J. Kim, and M. Ree, *Macromolecules*, **37**, 4174 (2004). (e) T. J. Shin and M. Ree, *J. Phys. Chem. B*, **111**, 13894 (2007). (f) K. Heo, J. Yoon, K. S. Jin, S. Jin, H. Sato, Y. Ozaki, M. M. Satkowski, I. Noda, and M. Ree, *J. Phys. Chem. B*, **112**, 4571 (2008).

(22) (a) B. Lee, I. Park, J. Yoon, S. Park, J. Kim, K.-W. Kim, T. Chang, and M. Ree, *Macromolecules*, **38**, 4311 (2005). (b) I. Park, B. Lee, J. Ryu, K. Im, J. Yoon, M. Ree, and T. Chang,

*Macromolecules,* **38**, 10532 (2005). (c) K. Heo, J. Yoon, and M. Ree, *IEE Proc. Bionanotechnology,* **153**, 121 (2006). (d) S. Jin, J. Yoon, K. Heo, H.-W. Park, T. J. Shin, T. Chang, and M. Ree, *J. Appl. Cryst.*, **40**, 950 (2007). (e) K. Heo, S.-G. Park, J. Yoon, K. S. Jin, S. Jin, S.-W. Rhee, and M. Ree, *J. Phys. Chem. C*, **111**, 10848 (2007). (f) K. Heo, J. Yoon, K. S. Jin, S. Jin, G. Kim, H. Sato, Y. Ozaki, M. M. Satkowski, I. Noda, and M. Ree, *J. Appl. Cryst.*, **40**, s594 (2007). (g) J. Yoon, S. C. Choi, S. Jin, K. S. Jin, K. Heo, and M. Ree, *J. Appl. Cryst.*, **40**, s669 (2007). (h) K. Heo, K. S. Oh, J. Yoon, K. S. Jin, S. Jin, C. K. Choi, and M. Ree, *J. Appl. Cryst.*, **40**, s614 (2007). (i) T. J. Lee, G.-S. Byun, K. S. Jin, K. Heo, G. Kim, S. Y. Kim, I. Cho, and M. Ree, *J. Appl. Cryst.*, **40**, s620 (2007). (j) J. Yoon, S. Y. Yang, K. Heo, B. Lee, W. Joo, J. K. Kim, and M. Ree, *J. Appl. Cryst.*, **40**, 305 (2007). (k) K. Heo, J. Yoon, S. Jin, J. Kim, K.-W. Kim, T. J. Shin, B. Chung, T. Chang, and M. Ree, *J. Appl. Cryst.*, **41**, 281 (2008).

(23) (a) C.-J. Yu, J. Kim, K.-W. Kim, G.-H. Kim, H.-S. Lee, M. Ree, and K.-J. Kim, *J. Kor. Vac. Soc.*, **14**, 138 (2005). (b) D. S. Jang, H. J. Lee, B. Lee, B. H. Hong, H. J. Cha, J. Yoon, K. Lim, Y. J. Yoon, J. Kim, M. Ree, H. C. Lee, and K. Y. Choi, *FEBS Letters*, **280**, 4166 (2006). (c) J. M. Choi, S. Y. Kang, W. J. Bae, K. S. Jin, M. Ree, and Y. Cho, *J. Biol. Chem.*, **282**, 9941 (2007). (d) D. Y. Kim, K. S. Jin, E. Kwon, M. Ree, and K. K. Kim, *Proc. Natl. Acad. Sci. USA*, **104**, 8779 (2007). (e) J. H. Lee, G. B. Kang, H.-H. Lim, K. S. Jin, S.-H. Kim, M. Ree, C.-S. Park, S.-J. Kim, and S. H. Eom, *J. Mol. Biol.*, **376**, 308 (2008). (f) K. S. Jin, D. Y. Kim, Y. Rho, V. B. Le, E. Kwon, K. K. Kim, and M. Ree, *J. Synchrotron Rad.*, **15**, 219 (2008).

(24) M. Ree and I. S. Ko, *Phys. High Tech.*, **14**, 2 (2005).

(25) K. Kuwajima, T. Inobe, and M. Arai, *Macromol. Res.*, **14**, 166 (2006).

(26) W. T. Chuang, U. S. Jeng, H. S. Sheu, and P. D. Hong, *Macromol. Res.*, **14**, 45 (2006).

(27) C. Li, G. H. Li, H. C. Moon, D. H. Lee, J. K. Kim, and J. Cho, *Macromol. Res.*, **15**, 656 (2007).

(28) O. Glatter and O. Kratky, *Small Angle X-ray Scattering*, Academic Press, New York, 1982.

(29) R.-J. Roe, *Methods of X-Ray and Neutron Scattering in Polymer Science*, Oxford, U. Press, New York, 2000.

(30) F. Ganazzoli and R. La Ferla, *J. Chem. Phys.*, **113**, 9288 (2000).

(31) (a) O. Glatter, *Acta Phys. Austriaca*, **47**, 83 (1977). (b) O. Glatter, *J. Appl. Cryst.*, **10**, 415 (1977). (c) O. Glatter, *J. Appl. Cryst.*, **13**, 577 (1980).

(32) S. Rathgeber, M. Monkenbusch, M. Kreitschmann, V. Urban, and A. Brulet, *J. Chem. Phys.*, **117**, 4047 (2002).

(33) M. Daoud and J. Cotton, *J. Phys. (Paris)*, **43**, 531 (1982).

(34) D. Papanagopoulos and A. Dondos, *Eur. Polym. J.*, **40**, 2305 (2004).

(35) J. S. Pedersen, *Adv. Colloid Interf. Sci.*, **70**, 171 (1997).

(36) M. Kurata and Y. Tsunashima, in *Polymer Handbook,* 3rd ed., J. Brandrup and H. Immergut, Eds., Wiley-Interscience, New York, 1989, VII, pp. 33.